Assessing the damaging effects of railway dynamic wheel loads on railway foundations

Burrow, Michael; Jin, Shi; Wehbi, Mohamed; Ghataora, Gurmel

DOI:
10.3141/2607-09

Document Version
Peer reviewed version

Citation for published version (Harvard):
Burrow, M, Jin, S, Wehbi, M & Ghataora, G 2017, 'Assessing the damaging effects of railway dynamic wheel loads on railway foundations', *Transportation Research Record*, vol. 2607, no. 1, pp. 62-73. https://doi.org/10.3141/2607-09

Assessing the Damaging Effects of Railway Dynamic Wheel Loads on Railway Foundations

Burrow M. P. N. (PhD) (corresponding author)
Senior Lecturer
Department of Civil Engineering, the University of Birmingham, Birmingham, B15 2TT, UK, Tel: +44 121 4145079
e: m.p.n.burrow@bham.ac.uk

Jin Shi (PhD)
Associate Professor in Railway Engineering, Department of Road and Railway Engineering, Faculty of Civil Engineering, Beijing Jiaotong University, Beijing China 100044
School of Civil Engineering, Beijing Jiaotong University, Beijing, China
e: shijin-bjtu@hotmail.com

Wehbi, M. (PhD)
Senior Track Designer
Network Rail, The Mailbox, 100 Wharfside Street, Birmingham, West Midlands, B1 1RT
e: Mohamed.Wehbi@networkrail.co.uk

Ghataora, G.S. (PhD)
Senior Lecturer
Department of Civil Engineering, the University of Birmingham, Birmingham, B15 2TT, UK
Tel: +44 121 4145047
e: g.s.ghataora@bham.ac.uk

Word count: 5,221 words text + 3 tables + 6 figures x 250 words (each) = 7, 471 words

Submission date: 1st August, 2016
Re-submission date: 14th November, 2016

ABSTRACT

Dynamic train wheel loads, which can be significantly greater than static loads, occur due a variety of factors and unless they are properly considered in track structural design, significant unplanned maintenance and premature track failure may result. This is particularly so for traditional ballasted railways built on soft foundations because although ballast lends itself to maintenance, it is often problematic and costly to repair damaged foundations. To address this, a rigorous combined analytical-numerical approach is described to predict and characterize, for the first time, the damage to which railway foundations can be subjected as a result of dynamic loads. The approach marries a sophisticated three-dimensional dynamic model of the train-track system incorporating vertical track quality, foundation soil distress models, statistical analysis methods and results of field investigation.

The resulting analyses demonstrate that the magnitudes and distributions of dynamic loads are a function of train speed and track quality and that specific locations experience significantly higher amounts of damage which can lead to a variety of track faults. The approach is illustrated via a study of a heavy haul railway line in China where the wheel loads and tonnage carried are set to increase significantly. The study suggests that the thickness of the ballasted layer would need to increase by over 20% to prevent premature foundation failure provided that the track is maintained in good condition, and by significantly more should the track condition be allowed to deteriorate.

Keywords: Railway, dynamic loads, foundations, design

INTRODUCTION

The railway track is a structural system built to withstand the combined effects of traffic and the environment for a pre-determined period of time, so that railway vehicle operating and maintenance costs, passenger comfort and safety are kept within acceptable limits and the foundation is adequately protected. Dynamic train loads induced by track irregularities and vehicle characteristics can reduce significantly the life of the components of the structural system.

Although a number of international railway infrastructure operators have developed railway track structural design standards they do not adequately take into account the spatial fluctuating nature of dynamic loads [1]. By implication the use of these design standards may lead to the under design of the structural system, premature failure of track components and its foundation, unplanned maintenance, reduced safety and higher train operating costs.

To better understand the implications of dynamic loads on the railway system, considerable research has been undertaken to measure dynamic loads in the field and also to estimate, via laboratory analysis, their potential impacts on the deterioration of the railway structural system. Methods have also been proposed which if used provide a means for enabling the spectrum of dynamic train loads to be accounted for within railway track design, principally by Eisenman [2] and Stewart and O'Rourke [3].

The method suggested by Eisenman [2] is based on studies of measured dynamic loads and takes into account vehicle speed and track condition. For speeds of up to 60 km/h, Eisenman found that dynamic loads followed a Gaussian distribution with a mean value which was independent of the operating speed, V, but dependent on track condition, φ. At 60 km/h and above the dynamic forces were found to be a function of both vehicle speed track condition.

Stewart and O'Rourke's method [3] relies on field measurements of dynamic loads. For the analysis of the substructure they assume that a single load application comprises of the two axles of the trailing and two of the leading axles of a pair of coupled wagons. To calculate the distribution of the maximum loads, Stewart and O'Rourke assume that the maximum static train load acts on the outer two axles of the configuration, whilst the inner two axles impart a high dynamic load corresponding to a very low probability of occurrence (they suggest 0.01%) determined from the field data. When the effects of fatigue loading on the foundation are to be calculated, Stewart and O'Rourke suggest that a spectrum of loads should be determined from the distribution of field measured loads. To achieve this, they propose that the frequency distribution of measured loads should be divided into a number of bands of probability of occurrence (e.g. 0 - 5%, 5 – 10% etc.) and that a representative load application for design is determined for each.

The studies by Eisenman [2] and Stewart and O'Rourke [3] are based on empiricism, rely on field measurement, which can be time consuming and expensive, and they overlook a number of important factors. Both methods assume that the distribution of loads in the foundation matches that of the surface wheel load distribution. However, the mathematical relationship between the applied surface wheel load and the resulting damage to the foundation is non-linear and therefore the statistical distribution of component damage does not match that of the surface loads. Further, the deterioration at any point along the track structure depends on the accumulated damage due to each passing wheel load which can vary in magnitude depending on the proximity of a track irregularity. Dynamic loads due to track irregularities are likely to be highest in the vicinity of a particular track irregularity, where they are likely to occur repeatedly leading to increased rates of track deterioration at these locations.

Advances in computer modeling capability are enabling accurate and complex numerical models of the railway train-track system to be built. These if used carefully can better help to understand railway track system performance under dynamic loads in a variety of operating conditions, thereby reducing the need for potentially time consuming and costly field and laboratory trials. Numerical models have been developed to investigate a variety of track related issues

including those associated with the transition between stiff track structures and less stiff railway track [4-7], ground vibration [8, 9], seismic analysis [10], critical velocity [11] and the integrity of track components under dynamic loads [12-15].

However, very few numerical studies have been undertaken to investigate the relationships between dynamic wheel loads, track structural design and railway foundation deterioration along a section of railway track. To address this, this paper establishes a rational analytical-numerical procedure which enables dynamic wheel loads to be properly accounted for in the structural design of railway track, thereby preventing premature failure and unplanned maintenance. The procedure builds on that suggested for the analysis of highway distress [16]. It utilizes a three dimensional dynamic finite element model (FEM) of the railway train-track system incorporating track quality, foundation structural distress models and statistical analysis methods. The procedure is demonstrated via a case study of the Shuanghuang coal route in China.

THEORETICAL FRAMEWORK

The approach proposed consists of the following elements:

i) Structural distress models of the track foundation to determine the values of the critical stresses, strains and deflections in the materials which comprise the substructure as a function of the magnitude and number of load applications

ii) A 3-D dynamic FEM of the railway train-track system, incorporating a model of track quality variability, to enable stresses, strains and deflections to be computed as a function of dynamic train loads at specific locations in the track structural system (see Figure 1).

Structural distress models

Railway Foundation Failure Mechanisms

The track foundation becomes progressively damaged through the cumulative effects of traffic induced repetitions of stresses and strains. For fine-grained subgrade soils the resulting damage can manifest as progressive shear failure and / or an excessive rate of settlement [17]. Progressive shear failure occurs where cyclic stresses are sufficiently high and are applied for long enough to cause material to be sheared and remolded. An excessive rate of settlement occurs through plastic deformation of the subgrade and may cause a ballast pocket to form. For shear failure, the design problem can be considered to be putting a limiting value on the plastic strain, whereas for an excessive rate of settlement the design problem is to limit the amount of cumulative plastic deformation [17].

Distress models

For fine-grained subgrade soils, it is recognized that plastic strain is a function of the number of loading cycles, N, soil stress history and drainage conditions. Models to predict plastic strain, ε_p, in fine grained materials are typically of the following form [18]:

$$\varepsilon_p = CN^b \quad (1)$$

Where C is a constant related to the material properties.

To take into account soil physical state and type a modified version of Equation 2 has been suggested [17]:

$$\varepsilon_p = a\left(\frac{\sigma_d}{\sigma_s}\right)^m N^b \quad (2)$$

Where *a*, *b* and *m* are material parameters determined from experiment, σ_d is the deviator stress and σ_s is the soil static strength.

Noting that the permanent deformation, ρ, can be written as

$$\rho = \int_o^T \varepsilon_p ds \quad (3)$$

where *T* is the thickness of the foundation.

then:

$$\rho = \int_0^T A\left(\frac{\sigma_d}{\sigma_s}\right)^m N^b \quad (4)$$

Phenomological theory of cumulative damage

The phenomological theory of cumulative damage was advanced by Miner [19] to predict the fatigue life of materials subjected to fluctuating stress amplitudes. The theory states that the cumulative damage *D*, is the linear summation of damages, D_i, due to N_i applications at stress or strain level *i*:

$$D = \sum_{i=1}^{r} D_i = \sum_{i=1}^{r} \frac{N_i}{N_{f_i}} \quad (5)$$

Where N_{fi} is the number of applications to failure at stress, or strain, level *i*. Failure occurs when $D = 1$.

Using Equations 3 to 6, it is possible to estimate the proportion of the total life used at a location *k* on the railway track due to a single load application as follows:

For shear failure:

$$D_{sf(k)} = \sum_{j=1}^{N} \frac{1}{\left(\frac{\varepsilon_{Psf}}{a}\right)^{\frac{1}{b}}\left(\frac{\sigma_s}{\sigma_d}\right)^{\frac{m}{b}}} \quad (6)$$

where ε_{psf} is the plastic strain at failure.

For plastic settlement:

$$D_{pf(k)} = \sum_{j=1}^{N} \frac{1}{\left(\frac{\rho_{sf}}{A}\right)^{\frac{1}{b}} \int_0^T \left(\frac{\sigma_s}{\sigma_d}\right)^{\frac{m}{b}} dt} \quad (7)$$

where ρ_{sf}, is the amount of plastic deformation at failure.
For the application given below, the value of the parameters used in equations 6 and 7 are shown in Table 1, together with a description of how they were obtained.

APPLICATION

As part of China's solution to its current shortage of transport capacity it is increasing utilization on many of its heavy haul railway lines. One such line is the 588km long Shuanghuang railway, an important route in China's coal corridor, which runs from Shenchi in Shanxi province to the Huanghua port in Hebei province. The line currently carries between 30-40 million tonnes of coal annually at speeds of up to 75km/h. In order to satisfy predicted greater coal output the amount carried on the line is set to increase to 600 million tonnes/yr with an increase in train wheel loads from 125kN to 150kN [20].

An extensive research project was undertaken to investigate the implications of the proposed increases in tonnage and loads on safety, track component damage, track structural design and maintenance. As part of the project a plain line (tangent) section of an embankment section was instrumented with accelerometers during its construction to measure train-induced accelerations in the rail, ties and the embankment at various locations [4]. The work presented here examines, using the suggested analytical-numerical procedure, the implications of the proposed increases in traffic on track structural design and maintenance.

Numerical Model

A dynamic train-track FEM representing a train of wagons running on a plain line 100 m section of the embankment, incorporating a means to modify track quality, was built using the ABAQUS Explicit™ software. The model configuration of the model, consisting of 124, 357 elements and 176, 268 nodes, is shown in Figure 1Figure 1. The values of the material properties for each component of the model are given in Table 1 Material properties for modelling purposesThe track structure and vehicle models, the method used to incorporate track quality within the model and the model's validation are briefly described below.

Track structure

The rails, ties, ballast and embankment were represented using solid eight-node elements with the material properties given in Table 1. The track substructure was modelled as a layer of ballast underlain by three discrete layers of sand and gravel, engineering fill and silt sand respectively to represent the embankment's construction according to Chinese design standards [21].

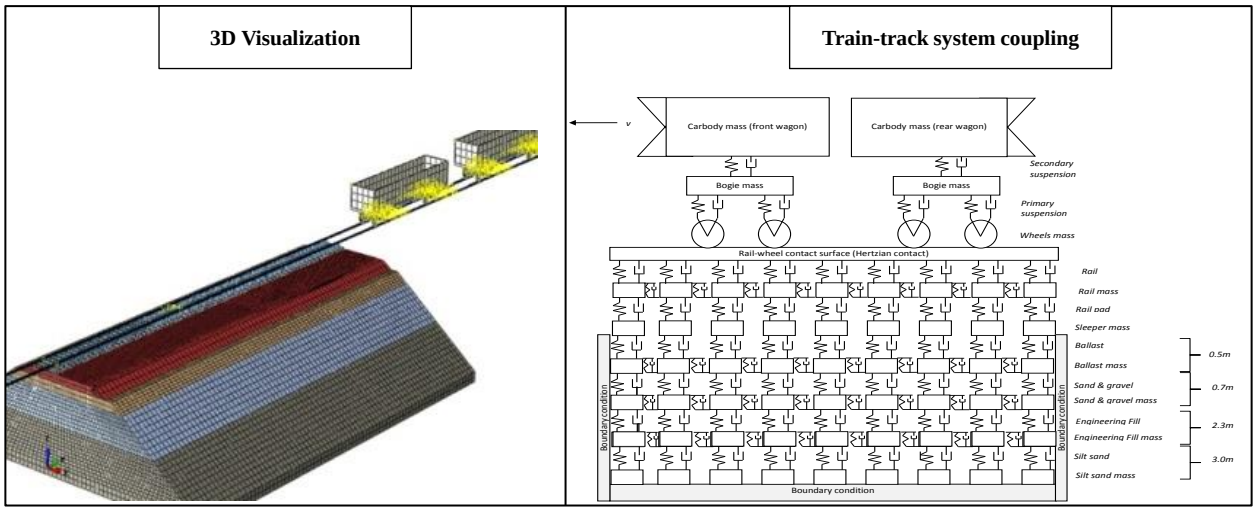

Figure 1 FEM representation of railway track system

Track quality

Three vertical track profiles representing good, fair and poor track quality according to the US Federal Railroad Administration classification system were represented within the FEM. The vertical profiles were characterized within the FEM using a one-sided power spectral density (PSD) function, $S_v(\Omega)$, suggested by Fries and Coffey [24]:

$$S_v(\Omega) = \frac{kA_v\Omega_c^2}{\Omega^2(\Omega^2 + \Omega_c^2)} \quad (8)$$

where Ω is the spatial frequency of the track irregularity (Hz), A_v is the roughness coefficient (cm^2.rad/m) and k is the safety coefficient. The values of the coefficients in Equation 8 which were used to represent the three track quality states are given in Table 1. The same profile was used for both rails.

254

Table 1 Material properties for modelling purposes

Component	Property	Value	Note
Freight Wagon	Mass of car body (Kg 10^3)	91.4	Two UIC Class T0AB freight wagons were modelled. The associated FEM parameters required for the FEM are as suggested by [22].
	Inertia of car body (Kg m^2)	1.33×10^5	
	Mass of bogie (Kg)	496	
	Inertia of bogie (Kg m^2)	190·	
	Mass of wheel (Kg)	1257	
	Primary suspension stiffness (MN/m)	13	
	Primary suspension damping (Ns/m)	3×10^5	
	Secondary suspension stiffness (MN/m)	4.4	
	Secondary suspension damping (Ns/m)	4×10^3	
Rail	Young's modulus, GPa	210	Parameters for the FEM chosen to match the type of rail installed in situ
	Poisson's ratio	0.3	
	Density kg/m^3	7830	
Tie	Young's modulus, GPa	35	From Chinese railway design standards: TB10001: 2005: [21]
	Poisson's ratio	0.22	
	Density kg/m^3	2600	
Fastener	Vertical stiffness, kN/mm	78	Values taken from those suggested by [9]`for the analysis of a heavy haul line in China built to similar standards
	Vertical damping kN.s/m	50	
	Horizontal stiffness, kN/mm	45	
	Horizontal damping ,kN.s/m	60	
Ballast (0.5m thick)	Resilient modulus, MPa	180	From Chinese railway design standards: TB10001: 2005: [21]. Note the ballast was assumed to be clean (i.e not fouled)
	Poisson's ratio	0.27	
	Density kg/m^3	1650	
Track quality* *Poor (FRA4) (max speed 96 km/h)*	Ω_c (cm^2.rad/m)	0.8245	Track quality is typically represented by a one-sided power spectral density (PSD) function in numerical models of the track system. For this study the PSD suggested by Fries and Coffey [23] was selected. The values of the coefficients Ω_c, A_v and k selected for each track quality state are those suggested by Fries and Coffey [23] to represent good, fair and poor track
	A_v (cm^2.rad/m)	0.5376	
	k	0.25	
	Amplitude (mm)	30~40	

	Moderate (FRA5) (max speed 128 km/h)	Ω_c (cm^2.rad/m)	0.8245	quality according to the US Federal Railroad Administration classification system.
		A_v (cm^2.rad/m)	0.2095	
		k	0.25	
		Amplitude (mm)	10~15	
	Good (FRA6) (max speed 176 km/h)	Ω_c (cm^2.rad/m)	0.8245	
		A_v (cm^2.rad/m)	0.0339	
		k	0.25	
		Amplitude (mm)	5~6	
Layer 1: Sand gravel (0.7 m thick)	*Parameters for FEM*	Resilient modulus MPa	180	Initial modulus values determined from plate loading tests conducted in-situ on the 100 m section of the Shuanghuang line used for the case study. Thereafter an iterative process was used to obtain the final resilient modulus values by successively modifying the resilient modulus values in each of the three layers until the accelerations given by the model matched field measurements [24].
		Poisson's ratio	0.3	
		Density kg/m^3	2300	
	Parameters for distress model	a	0.52	Determined from plastic deformation laboratory tests on material taken from the 100m section of the embankment on the Shuanghuang line used for the case study. Note although the material in layer 1 cannot be considered to be fine-grained, it was found that its permanent deformation characteristics could be modelled using an equation of the form given by Equation 7 [25]
		b	0.15	
		m	1.49	
		σ_s (KPa)	350	
Layer 2: Class A engineering fill (2.3 m thick)	*Parameters for FEM*	Resilient modulus, MPa	130	As for layer 1 [24].
		Poisson's ratio	0.3	
		Density kg/m^3	2100	
	Parameters for Distress model	a	0.85	As for layer 1 [25]
		b	0.14	
		m	1.49	
		σ_s , kPa	200	
Layer 3: Silty sand (3 m thick)	*Parameters for FEM*	Resilient modulus, MPa	50	As for layers 1 and 2 [24].
		Poisson's ratio, ν	0.25	
		Density kg/m^3	1800	

	a	0.64	As for layes 1 and 2 [25]
Parameters for	b	0.1	
Distress model	m	1.16	
	$\sigma_{s,}\ kPa$	100	

*Note that the maximum permitted amplitudes of track quality deviations on main-line heavy haul railway track in many countries is limited to between 6 – 10 mm.

Vehicle Model

In accordance with analytical railway foundation design convention, the railway freight vehicle was represented by the leading and trailing bogies of two coupled wagons [3]. The coupled wagons were modelled using a multibody system consisting of a car body, bolster, frame and wheelset (Figure 1). The primary suspension system, connecting the wheels and the frame, and the secondary system were modelled using a series of linear springs and viscous dashpots. The rail-wheel interaction in the normal direction was modelled as a Hertzian contact (where separation is allowed resulting in a zero contact force), since it is widely used in FE analyses to represent the contact between spherical objects and deformable surfaces (such as the wheel and the rail respectively in railway applications [9]). Hertzian contact assumes that the contact surface between the wheel and rail increases as the deformation increases. The normal contact force *P(t)* can be determined as follows [9]:

$$P(t) = \left[\frac{1}{G}\Delta Z(t)\right]^{\frac{3}{2}} \quad (9)$$

where $\Delta Z(t)$ is the elastic compression between the rail and wheel (m). The contact constant G is given by $G = 3.86R^{-0.115} \times 10^{-8}$ m/N$^{3/2}$ where *R* is the wheel radius. The wheel-rail creep force, τ_{crit}, is given by:

$$\tau_{crit} = \mu P \quad (10)$$

where μ is the coefficient of friction between the rail and the wheel.

To quantify the effects of fluctuating dynamic wheel loads, the maximum stresses due to the passage of a train were computed at discrete sections along the track sufficiently short in length to enable the peak stresses to be determined. The principle of superposition was used to calculate the effect of a train of wagons. It was found that superimposing the loads in this way increased the stresses by less than 5% compared to calculating the stresses due only to the two coupled wagons.

Model validation

To provide confidence in the outputs of the developed FEM, computed and field measured and accelerations and vibrations were compared at various positions in the track structure for a train travelling at 71 km/h [4]. Since the embankment section has been newly constructed the track quality in the FEM was considered to be perfectly smooth. Table 3 shows that the computed and measured values are generally in good agreement, albeit that the computed values are slightly higher. A reason for the slightly higher computed values could be attributed to the heavy rainfall which occurred just before the vibration and acceleration measurements, but after the field tests which were carried out to determine the properties of the materials in the embankment (see Table 1).

Table 2: Comparison of modelled and field measured accelerations and vibrations

	Accelerations (max) (g)		Vibration (dB)	
	Computed	Field	Computed	Field
Rail	40.00	23-50	155.0	153.7
Ties	10.00	3-11	147.1	138.0
Foundation surface	1.0	0.3-0.8	109.6	102.5
Foundation at 2m depth	0.40	0.4-0.6	105.0	100.5

ANALYSIS

Using the FEM and distress models described above, the maximum wheel force time histories and maximum stress time histories were calculated at discrete locations along and within the modelled embankment for a train of wagons with wheel loads of 125kN and 150kN travelling at speeds between 50 and 250km/h. Since the highest peak dynamic forces, and therefore the initiation of defects are likely to occur in the vicinity of specific track quality irregularities which cause large dynamic loads, damage was related to the area of track which becomes significantly damaged [16]. Track which is significantly damaged was assumed to be that subject to loads greater than the 95th, 98th and 99th percentile values.

Wheel forces

Figure 2 shows the distribution of the magnitude of the maximum wheel forces at discrete sections along the embankment for a train of wagons with nominal wheel loads of 125kN travelling at 75km/h with the three track quality profiles. The distribution results from a combination of the variability in track quality and the presence of ties which cause the stiffness of the track system to vary along the track. The variability apparent in the distribution of loads reduces as the track quality improves, corroborating Eisenman's experimental findings [2].

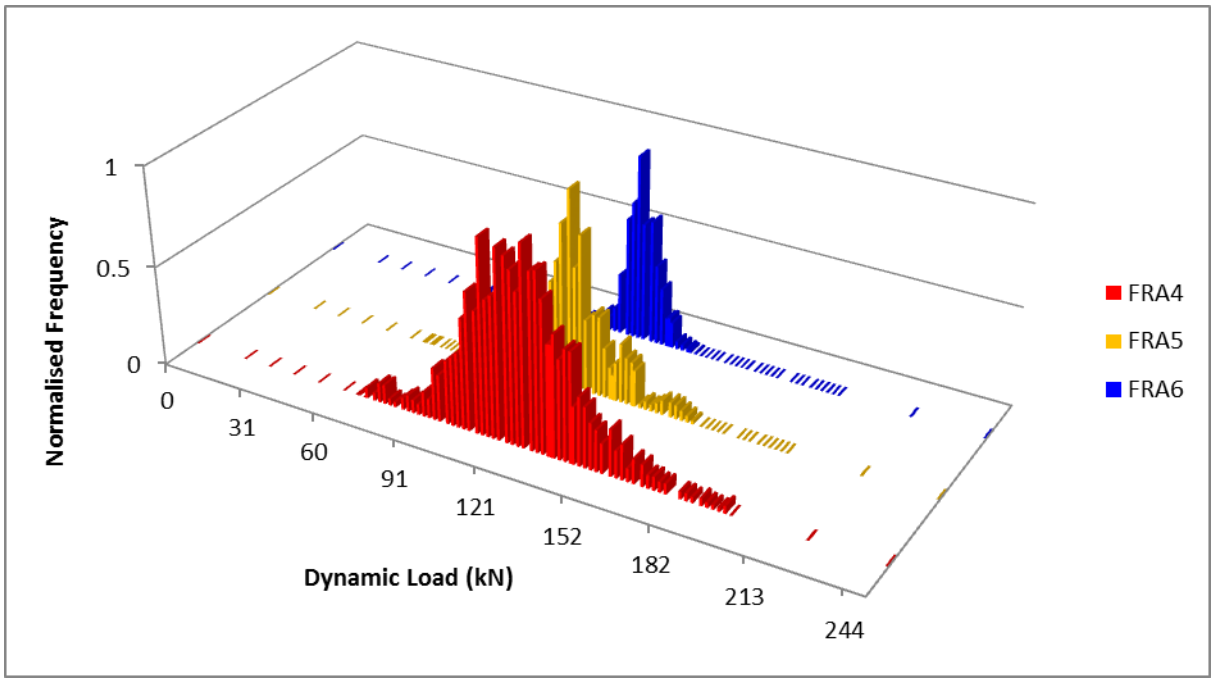

Figure 2 Dynamic rail force distribution at a speed of 75 km/h

To demonstrate the effect of speed and track quality on the magnitude of the maximum wheel loads, Figure 3 shows the 95th, 98th and 99th wheel forces (normalized by the static wheel load) as a function of vehicle speed and track condition. As might be expected, the dynamic wheel load increases with both train speed and deteriorated track. For example, when the track quality is in good condition and for train speeds of 50km/h, 2% of the track experiences dynamic wheel loads of between 15%-20% greater than the static wheel load. For speeds of 250km/h the dynamic forces are between 35%-45% greater than for the static case. When the track quality is in poor condition the corresponding load increases are 44%-52% and 125%-205% respectively.

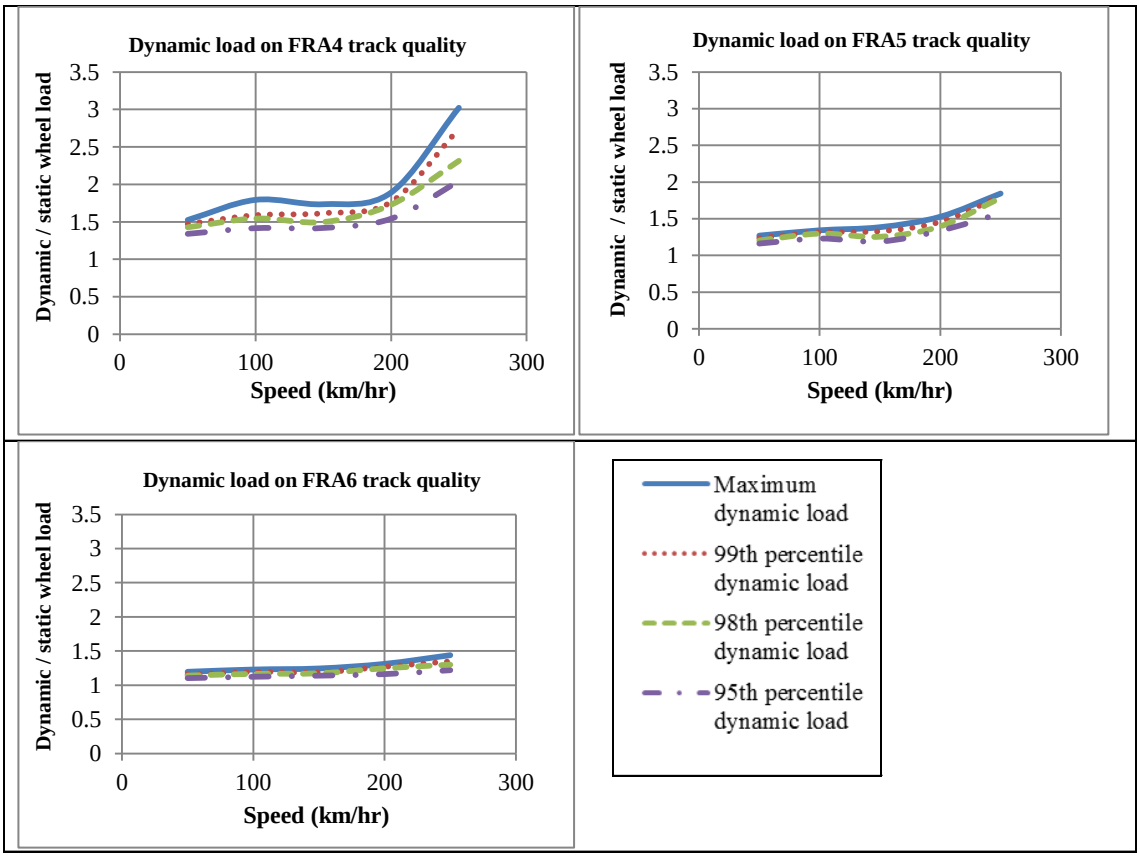

Figure 3 Dynamic wheel force vs. speed

Figure 3 shows a local maximum dynamic load for all three track conditions at a vehicle speed of approximately 100km/h. For perfectly smooth track the critical speed is that which results in a wheel encountering a tie at a frequency which matches the resonant frequency of the track structural system [11]. This frequency is known as the tie-passing frequency. When this phenomenon occurs, the response of the track to successive loading cycles are in-phase resulting in an amplified track response. For imperfect track, Figure 3 shows that the magnitude of the amplified response is also related to the quality of the track and therefore the magnitude of the dynamic loads. The effect of resonance is particularly apparent for the poorest track quality (FRA4) when the amplitudes of the most extreme dynamic loads caused by the presence of large track irregularities are sufficient for the resonance to be apparent. The resonant frequency can vary from 30Hz to 2000Hz depending on a number of factors including [26]:

1. Vehicle characteristics:
    a. Wheels, bogie and wagon spacing
    b. Sprung and un-sprung mass, primary and secondary stiffness and damping
2. Track properties:
    a. Track stiffness and damping of the different track components.
    b. The mass of the track structure, i.e. ballast, sub-ballast and subgrade.
    c. Tie spacing

Permanent strain and settlement in the embankment

The proportion of the amount of the life used by a single passage of the coupled wagon system in the three layers of the embankment was determined using equations 6 and 7 respectively. In accordance with the literature, permanent strain of 2% and 25mm of settlement in the embankment were taken to indicate failure according to the two measures of damage [27]. For a train travelling at 75km/h, the distribution in the Class A Engineering Fill layer of the embankment (i.e. the second layer) of fatigue life usage according to the strain and settlement criteria is shown in Figure 4.

In general it can be seen from Figure 4 that the variability and magnitude of the damage increases as the track quality decreases. It is also apparent that some sections along the embankment are subject to much greater damage than others (i.e. those sections which are in the vicinity of a particular irregularity). For example, for the second layer of the embankment when the track is in good condition the computed 99^{th} percentile value of strain damage is approximately 1.7 times greater than the computed median value and 2.3 times greater than the median value when the track is in poor condition. Similarly, for the settlement criterion the 99^{th} percentile value is approximately 1.4 times greater than the median value when the track is in good condition and 2.8 times greater when the track is in poor condition.

Assuming the train and track operating conditions remain unchanged the same sections of track will experience these greater amounts of damage for every load cycle over the life of the track. The resulting localized settlement is likely to cause increased dynamic loads in the same vicinity thus accelerating further the accrued damage. An example is the occurrence of localized failures, such as wet spots which can become apparent on railways built on soft foundations. Wet spots are caused by the upward migration of fines into the ballast under dynamic loads leading to ballast fouling and poorly performing ballast. The resulting non-homogenous railway track stiffness leads to worsening track quality which will increase further the magnitude of dynamic.

Constant tie spacing can result in resonance as mentioned above and therefore varying the spacing between ties could be a means of reducing localized track deterioration. In practice however, this is impractical for many railway infrastructure operators who use automated tie relaying systems and tamping machines. In the UK, for example, the practice is only employed at problematic sites where tie spacing is varied manually by +/- 5%. The approach advocated here can also be used to investigate alternative approaches to avoid resonance, such as determining permissible ranges of speeds at which specific types of vehicle can travel on particular sections of track.

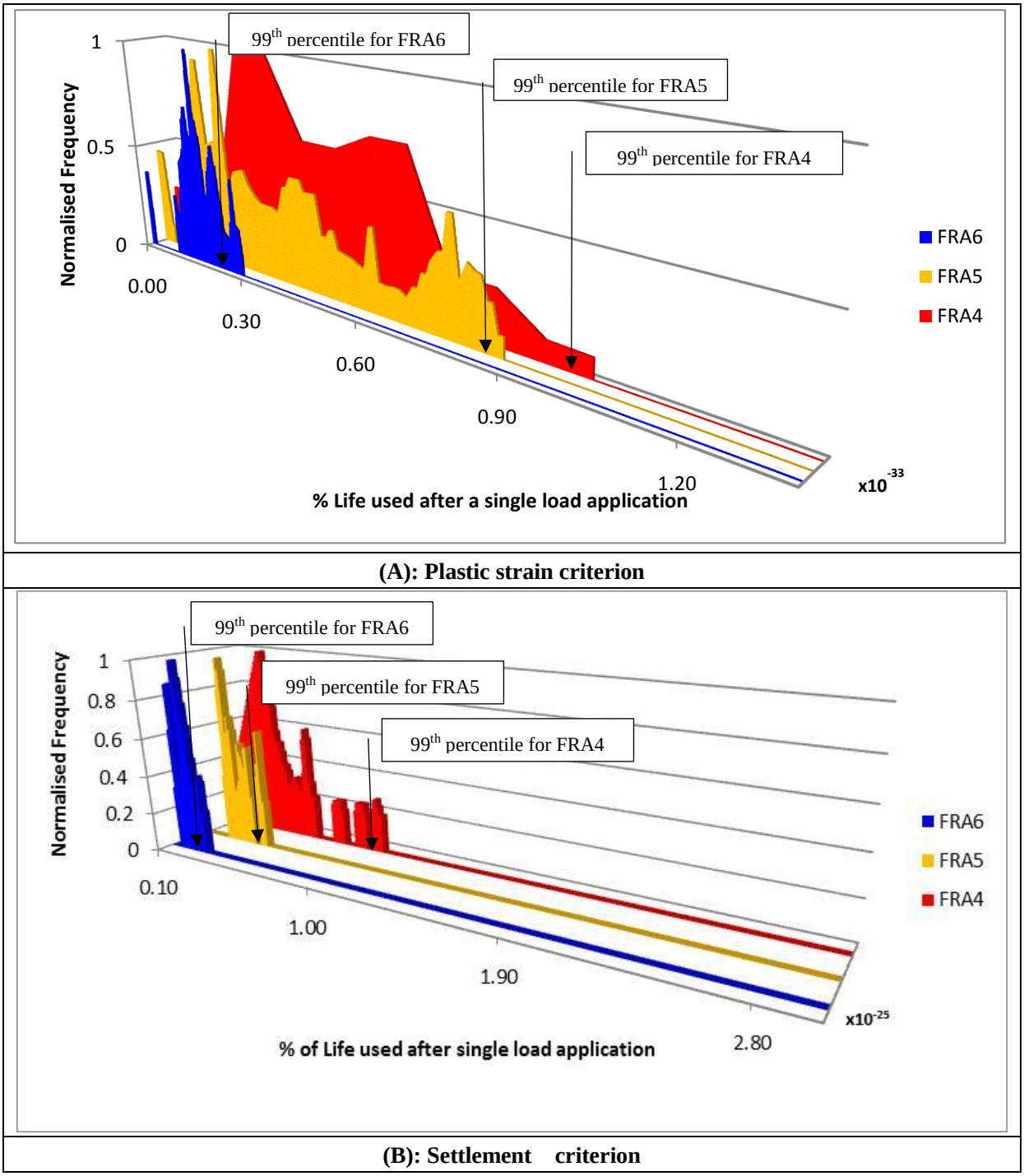

Figure 4 Distribution of fatigue life usage (damage) in second layer of embankment at a speed of 75 km/h

The 95th, 98th, 99th and 100th percentile computed fatigue life usage for a single passage of the coupled wagon system as a function of speed and track condition, are shown in Figure 5 and Figure 6 according to the strain and settlement measures of damage. In both figures the values have been normalized by the fatigue life by the application of a single static load. The resonance effect is evident at vehicle speeds of approximately 100km/h.

As may be expected the damage in the second layer of the embankment increases with both train speed and reduced track condition. For example, when the track quality is in good condition (FRA6) and for train speeds of 50km/h, 5% of the area of second layer of the embankment is subject to between 3-4 times the plastic strain than would be caused by a static train load. For speeds of 100km/h, 5% of the area of the second layer is subject to levels of plastic strain which are between 6-8.5 times greater than caused by a static load. For track in poor condition (FRA4) the corresponding computed increases in plastic strain are between 14-20 (50 km/h) and 300-450 (100 km/h) times respectively. Similar results can be observed for the permanent settlement measure of damage.

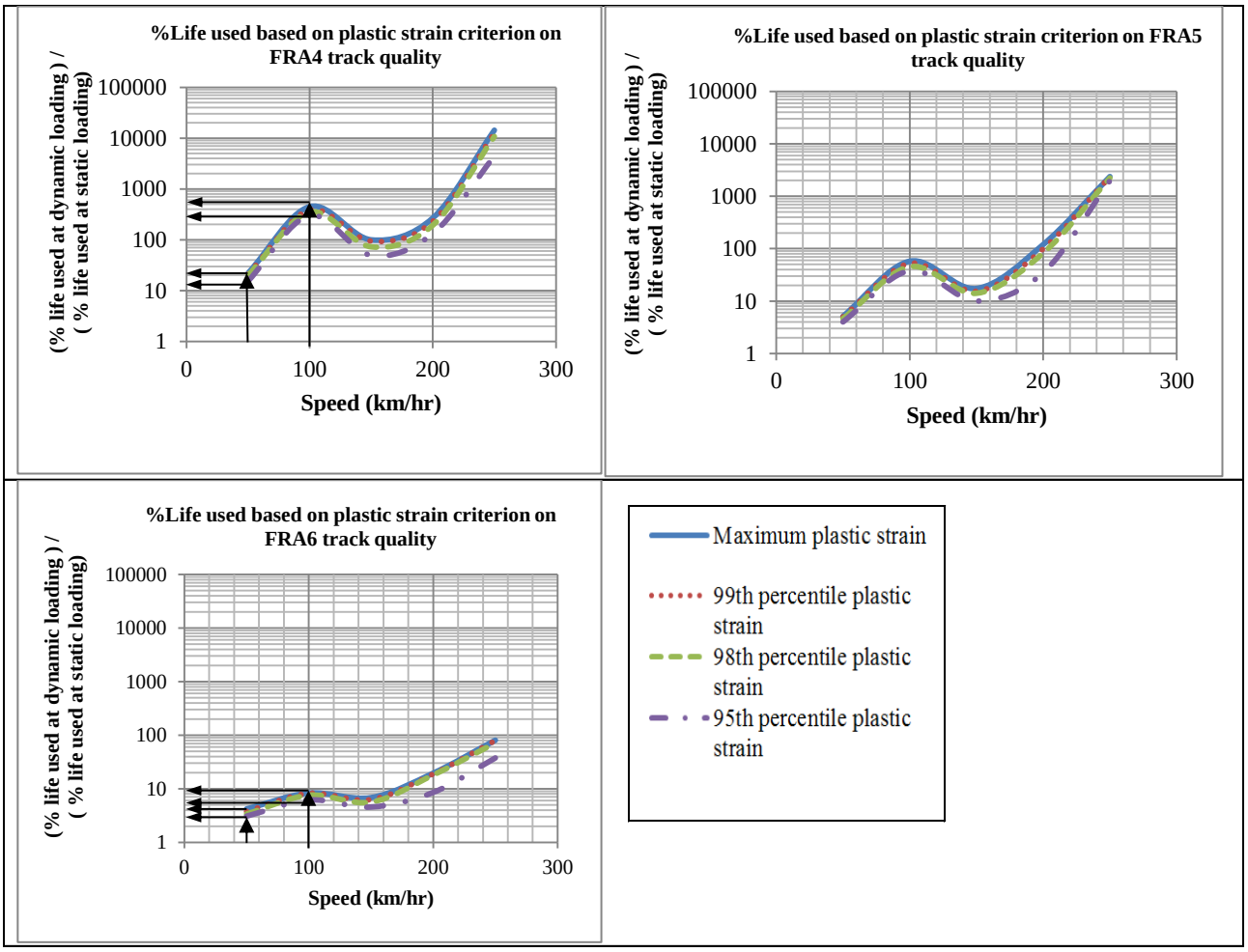

Figure 5 Plastic strain vs. speed (second layer of the embankment)

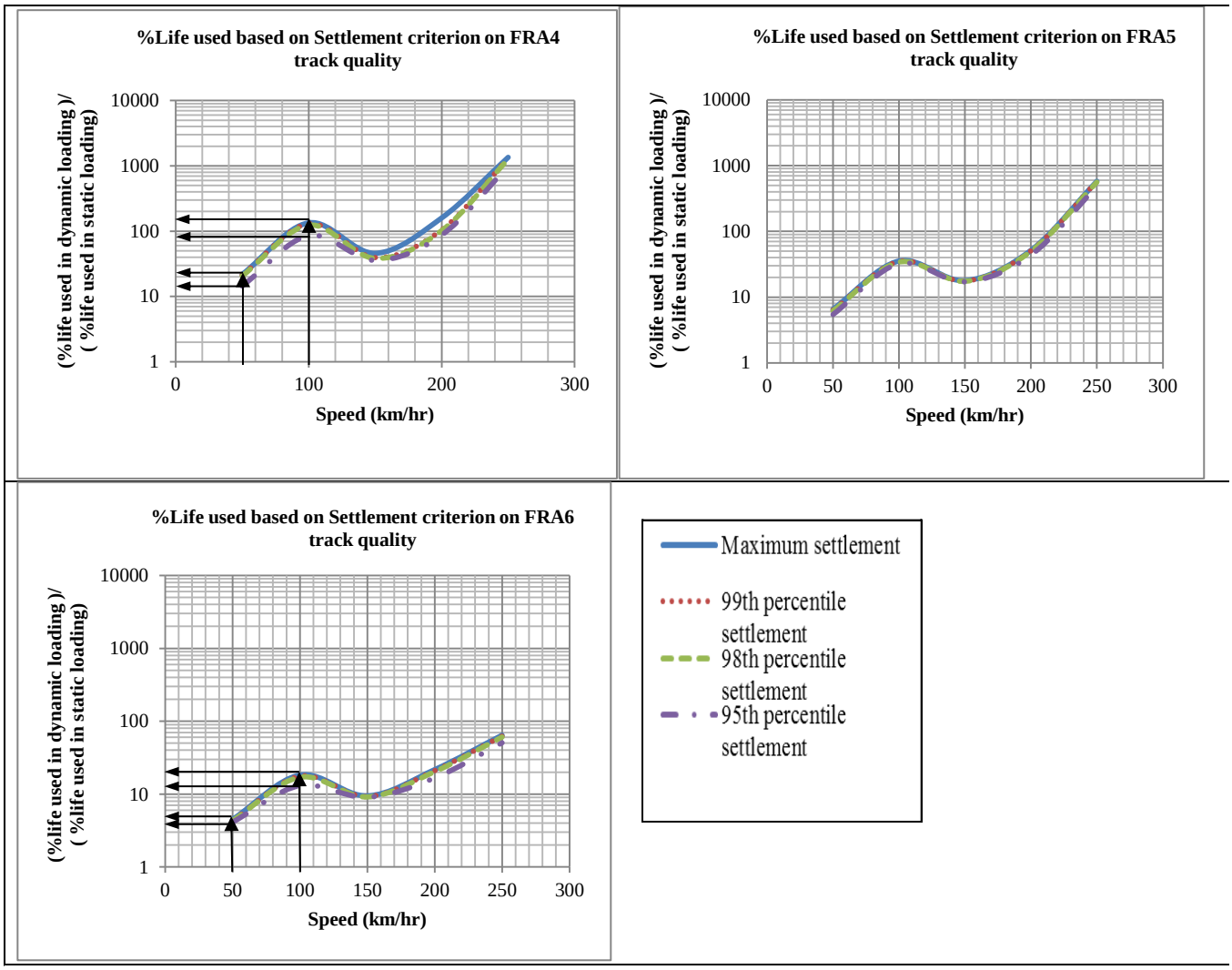

Figure 6 Total settlement vs. speed (second layer of the embankment)

APPLICATION

To demonstrate the implications of the proposed changes to the Shuanghuang line an analysis was carried out to compare the number of load cycles which each layer in the embankment could further undergo before failure. This analysis considered the plastic strain criterion under the following regimes:

1. Existing regime (i.e. 40MGT/yr for trains with wheel loads of 125kN for another 90 years. This is equivalent to $\frac{40\times10^6\times10^3\times90}{125/10\times8} = 3.6\times10^{10}$ load cycles (assuming 1 load cycle in the subgrade comprises of the leading and trailing axle axles of two adjacent wagons.)
2. The proposed regime for the remaining 90 years of the life of the track (i.e. 600MGT/yr with wheel loads of 150kN which is equivalent to $\frac{600\times10^6\times10^3\times90}{150/10\times8} = 4.5\times10^{11}$ load cycles).

For the two regimes, the ballast was considered to be clean throughout the analysis. The fractions of the remaining number of cycles to failure of each layer was calculated using Equation 6 and are shown in Table 3 normalized by the desired number of loading cycles. Under current operating conditions, Table 3 shows that for all track speeds considered, except for 150km/h, when the track quality is in a poor or fair condition the material in the second layer of the embankment would fail prematurely. From Table 3 it can also be seen that for the proposed heavier wheel load regime the second layer would fail prematurely no matter the train speed or track condition. The upper layer of the embankment would also fail prematurely if the condition of the track was maintained to anything other than a good condition, except for the case where the train speed is limited to 75km/h. The effect of travelling at the critical speed on the reduction in the life of the material in the embankment is also evident for the heavier wheel load.

The consequence of ballast maintenance on track life is evident by comparing the remaining life under the three track conditions modeled. For example, the second layer will last between 4-8 times longer, depending on the speed of the train, if the track is in a good condition (FRA6) compared to a fair condition (FRA5).

A further analysis determined the amount of additional granular material (ballast/sub-ballast) required to reduce the deviator stress in the Engineering Fill layer so that 99% of the track would not exceed the allowable fatigue life values. The resulting thicknesses are given in Table 3 and demonstrate that significant additional amounts of granular material would be required under the existing regime for all speeds if the track is not maintained in a good condition. Should the proposed changes to the capacity of the line take place, then the study suggests that an additional thickness of at least 110mm of the granular layer would be required, provided that the track is maintained in good condition.

Table 3: Remaining number of cycles to failure (according to plastic strain criteria) and additional ballast thickness requirements

	Sand / gravel layer						Engineering fill layer						Silty sand layer						Additional granular layer (mm)					
	FRA4		FRA5		FRA6		FRA4		FRA5		FRA6		FRA4		FRA5		FRA6		FRA4		FRA5		FRA6	
Load (kN) / Speed (km/h)	125	150	125	150	125	150	125	150	125	150	125	150	125	150	125	150	125	150	125	150	125	150	125	150
75	8.58	0.66	41.2	1.87	123	5.06	0.13	0.009	0.64	0.03	2.29	0.12	2480	32.1	12500	114	45300	419	105	280	20	185	0	110
100	2.43	0.19	13.8	0.63	81.25	3.33	0.02	0.002	0.22	0.01	1.61	0.08	368	4.78	3700	33.8	27000	251	220	420	75	260	0	130
125	5.55	0.21	29.3	0.69	113	3.56	0.06	0.003	0.55	0.01	2.03	0.06	263	4.02	2420	18.8	8900	88.2	160	375	25	250	0	150
150	13.68	0.24	66.5	0.76	160	3.80	0.18	0.004	1.52	0.01	2.58	0.04	191	3.38	1570	10.3	2680	30.9	90	335	0	245	0	175
175	8.33	0.15	25.8	0.30	97.25	2.12	0.12	0.003	0.54	0.00	1.38	0.02	92	1.63	398	2.62	1020	13.4	110	365	26	320	0	205

CONCLUSIONS

A novel rigorous analytical-numerical approach has been provided to take into account the spatial fluctuating nature of dynamic wheel loads within railway track structural design methods. Such an approach helps to ensure the adequate design of the structural system and thus facilitates the safe operation of the railway track, prevents premature track failure and therefore unplanned maintenance, and reduces train operating costs.

A number of conclusions may be drawn from the study as follows:

1. The magnitude of dynamic loads is a function of the train speed, axle load and track quality and specific locations along the track, corresponding to areas of poorer track quality, experience significantly higher dynamic loads. A natural frequency of vibration of the track structure was identified which corresponds to the tie passing frequency and is a function of the magnitude and wavelength of track irregularities.
2. The importance of ensuring good track quality is evident. Increased dynamic loads resulting from poor track quality can lead to localized increased rates of foundation deterioration and may lead to other types of track failure. This can cause a cycle of worsening track quality which in turn increases the localized dynamic loads.
3. The case study analysis of the Shuanghuang line, although relatively simplistic in that it assumed amongst other things constant train speed and track quality condition over time, showed that, provided that the track is maintained in good condition, an additional 20% of granular layer material would be required to prevent premature embankment failure.

A number of other causes of dynamic loads could be considered within an enhanced version of the model, thereby further increasing the accuracy of any analysis. These include out of round wheels, rail irregularities, fouled ballast and hanging ties. Furthermore it is recognized that the approach advocated requires the use of a number of parameters associated with the FEM and the deterioration models which need to be selected carefully for the conditions at hand.

ACKNOWLEDGEMENTS

The University of Birmingham’s Department of Civil Engineering and Centre for Railway Research and Education are thanked for providing facilities to carry out the research. The computations described in this paper were performed using the University of Birmingham's BlueBEAR HPC service, purchased through HEFCE SRIF-3 funds. Chinese central universities’ funds (2014JBZ011) were used to facilitate the research.

REFERENCES

1. Burrow, M.P.N., Bowness D. and Ghataora, G.S. (2007). A comparison of railway track foundation design methods. Proc. IMechE Part F: J. Rail and Rapid Transit. Vol 221, No F1, pp 1 – 12.
2. Eisenmann, J. (1992). Railway track foundation dynamics. Railway Engineering International Edition. No. 2, 17-20
3. Stewart, H.E. and O’Rourke, T.D. (1988). Load factor method for dynamic track loadings. Journal of Transportation Engineering, ASCE, 114(1).
4. Shi J., Burrow M.P.N., Chan, A.H.C. and Wang, Y.J. (2013). Measurements and simulation of the dynamic responses of a bridge-embankment transition zone below a heavy haul railway line. Proc IMechE, Part F: J. Rail Rapid Transit; 227(3): 254–268.

5. Gallego Giner, I., Lopez Pita, A., Vieira Chaves, E., and Rivas Alvarez, A. (2011). Design of embankment–structure transitions for railway infrastructure. Proceedings of the Institution of Civil Engineers. Transport 165, TR1, 27–37
6. Lei, X., and Zhang, B. (2010). Influence of track stiffness distribution on vehicle and track interactions in track transition. Proc. IMechE, Part F: J. Rail and Rapid Transit, 224(1), 592–604.
7. Andersson C. and Dahlberg T. (2000). Load impacts at railway turnout crossing. Vehicle System Dynamics, Vol 33, 131-142.
8. Ju, S.H., Liao, J.A. and Ye, Y.L. (2009). Behavior of ground vibration induced by trains moving on embankments with rail roughness. Soil Dynamics and Earthquake Engineering, 20: 1237-1249.
9. Zhai, W.M., Wang, K.Y., and Lin, J.H. (2007). Modeling and experiment of railway ballast vibrations. J. Sound Vibr, 270(4), 673–683.
10. Morteza, E. and Noghabi, H.H. (2013). Investigating Seismic Behavior of Ballasted Railway Track in Earthquake Excitation using Finite-Element Model in Three-Dimensional Space. Journal of Transportation Engineering, 139(7), 697-708
11. Ferrara, R., G. Leonardi, G. and Jourdan F (2013). A Two-Dimensional Numerical Model to Analyze the Critical Velocity of High Speed Infrastructure. Proceedings of the fourteenth international conference on civil, structural and environmental engineering computing. Cagliari, Sardinia, Italy.
12. Witt, S. (2008). The Influence of under sleeper pads on railway track dynamics. Report LIU-IEI-A—08/00442-SE. Linköping University, Sweden
13. Yang, L.A., Powrie, W., and Priest, J.A (2009). Dynamic stress analysis of a ballasted railway track bed during train passage. Journal of Geotechnical and Geoenvironmental Engineering, 135(5), 680–689.
14. Shi. J., Chan, A.C, and Burrow, M.P.N. (2013b). Influence of unsupported sleepers on the dynamic response of a heavy haul railway embankment. Proc IMechE, Part F: J. Rail and Rapid Transit; 227(6): 656-666.
15. Lundqvist A. and Dahlberg T. (2005). Load impact on railway track due to unsupported sleepers. Proc. IMechE, Part F. Journal of Rail and Rapid Transit,219, 31-40
16. Cebon, D. (2000). Handbook of Vehicle-Road Interaction. Taylor and Francis.
17. Li, D. and Selig, E.T. (1996). Cumulative plastic deformation for fine grained soils. Journal of Geotechnical Engineering, ASCE, 122(12).
18. Monismith, C.L., Ogawa, N., and Freeme, C.R. (1975). Permanent deformation characteristics of subgrade soils due to repeated loading. TRR. No. 537, TRB, Washington, D.C., 1-17.
19. Miner, M.A., (1945). Cumulative Damage in Fatigue. J. Applied Mechanics, 12, A159-A164.
20. Smith, K. (2013). Meeting China's burning desire for coal. International Railway Journal, August, 2913.
21. The Ministry of Railways of the People's Republic of China. (2005). Design Specification for Railway Foundations (TB10001-2005). China Railway Press, Beijing.
22. D. Ribeiroa, D., Calçadab, R. Delgadob, R., Brehmc, M. and Zabeld, V. (2013). Finite-element model calibration of a railway vehicle based on experimental modal parameters. Taylor & Francis: Vehicle System Dynamics, 51(6), p. 821–856.
23. Fries, R.H., and Coffey, B.M. (1990). A state-space approach to the synthesis of random vertical and crosslevel rail irregularities. J. Dyn. Syst., Measurement, and Control, 112(1), 83-87.

547 24. Dong, L and Zhao CG. Method for the dynamic response of subgrade subjected to
548 high-speed moving load. Engng Mech 2005; 25(11): 231–240.
549 25. Dong, L, Cai DG, Ye YS, Zhang QL and Zhao CG (2010). A method for predicting the
550 cumulative deformation of high-speed railway subgrades under cyclic train loads. China
551 Civil Engineering Journal; 43(6): 100–108.
552 26. Man, D., (2000). Pin-pin resonance as a reference in determining ballasted railway track
553 vibration behaviour. HERON Special issue: Dynamics of structures, 45(1).
554 27. Li, D. and Selig, E.T. (1998). Method for railroad track foundation design. I: Development. J.
555 Geotechnical and Geoenvironmental Engineering, ASCE, 124(4), 316-322.
556 28. Ghataora, G.S. and Burrow, M.P.N. (2010). Railway Foundations. In Geotechnical
557 Engineering Handbook. J. Ross Publishing.